Constraints on the Temperature and Composition of the Base of the Mantle

MICHAEL E. WYSESSION,[1] CRAIG R. BINA AND EMILE A. OKAL

Department of Geological Sciences, Northwestern University, Evanston, Illinois

P and *S* waves diffracted around the core-mantle boundary (CMB) are examined to obtain measurements of long-wavelength average velocities in D″, the base of the mantle. Observations are made of profiles of diffracted waves (*Sd* and *Pd*) from WWSSN and Canadian stations, and are compared to synthetic seismograms generated with the reflectivity method. The apparent ray parameters of the data and synthetic profiles serve as the basis of comparisons, which suggest significant lateral heterogeneity on the order of about 4% for both *P* and *S* velocities at the base of the mantle. While most of the D″ average velocity anomalies are on the order of ± 1% relative to PREM, our range in seismic heterogeneity is largely the result of a 3% *S* and *P* velocity low in D″ beneath Indonesia, which is made even more unusual by the fact that it is adjacent to a regional fast velocity anomaly beneath Southeast Asia. This velocity low is over a major rising plume in the outer core, as calculated by *Voorhies* [1986], and if this plume has been held in place over time through core-mantle coupling then the low velocity would be expected due to the increased mantle influx of heat and iron. We undertake a calculation of the variations in D″ seismic velocities due to changes in temperature and composition using a third-order Birch-Murnaghan equation of state with current available thermoelastic data on perovskite and magnesiowüstite. Using this model, small seismic velocity anomalies in D″ could be the result of temperature variations, though small fluctuations in relative amounts of magnesium and iron would have a greater effect on the velocities. For example, the Indonesian anomaly cannot be explained by only a thermal anomaly, but requires only a 20% increase in the Fe/(Mg+Fe) ratio (and even less if accompanied by a raise in temperature). In some regions of D″ the *P* and *S* velocities do not vary in tandem, as under Northern North America, where shear velocities are fast but *P* velocities are slightly slow. The implied lateral change in Poisson ratio could be the result of variations in the relative amounts of silicates and oxides, exacerbated by the high thermal gradients that are expected to exist in D″.

INTRODUCTION

In examining the structure of D″ (the very base of the mantle) the combined use of both *P* and *S* velocities supplies a greater constraint than only one or the other, and this is true as well with waves that diffract around the CMB. In *Wysession and Okal* [1988, 1989] we looked at the diffracted *Sd* and *Pd* waves separately, beginning to map out lateral heterogeneities in D″. What we present here is a joint examination of profiles of both *Pd* and *Sd* waves, facilitated with the use of reflectivity synthetic seismograms, which can model both arrivals at the same frequency levels. These diffracted wave profiles give us long wavelength information about the velocities in D″, and combined with the results from other disciplines (geomagnetics, in particular) we can begin to suggest and identify dynamic processes occurring in particular regions at the base of the mantle.

Mineral physics, especially the breakthroughs of recent experimental work, has begun to give us a thermochemical description of the materials (i.e., perovskite, magnesiowüstite) that comprise the lower mantle. It is therefore possible to begin comparing the seismic velocity anomalies observed with those predicted from thermoelastic principles. In this light, we will also attempt to compare the seismic velocity variations we find with those calculated from Birch-Murnaghan equations of state, using as initial parameters the recent results of mineral physics experiments.

Diffracted waves have long been identified as being as important tools for examining the CMB, as they can travel for thousands of km along the base of the mantle (shown in Figure 1). A careful examination of diffracted arrivals travelling along a similar azimuth to several stations from a single earthquake gives a good indication of the average velocity of that strip of D″ within which all the waves travel, once corrections are made so that we have removed all other effects, and a comparison is made with synthetic seismograms modeling identical earthquake-station geometries. These velocities, when compiled as a map for D″, will serve as the

[1]Now at Department of Earth and Planetary Sciences, Washington University, St. Louis, Missouri.

Dynamics of Earth's Deep Interior and Earth Rotation
Geophysical Monograph 72, IUGG Volume 12

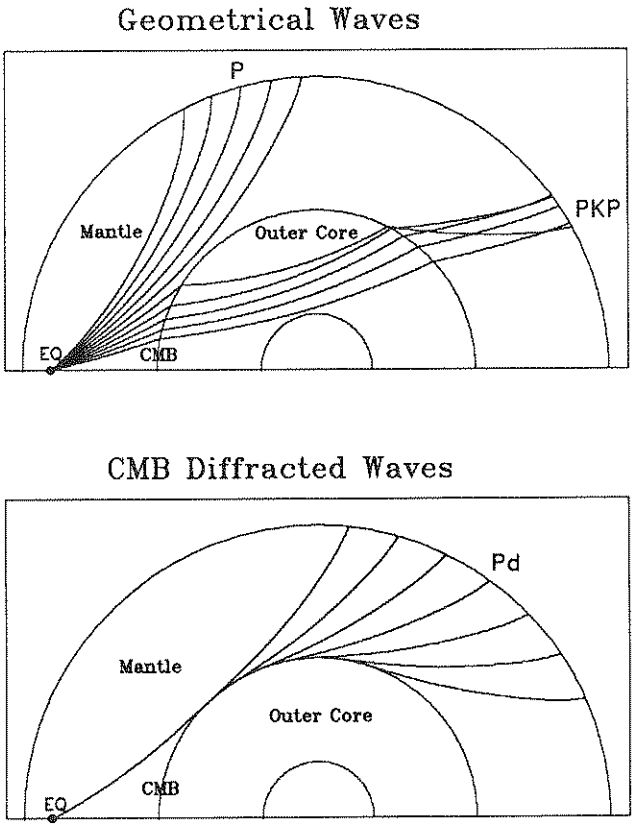

Figure 1. A demonstration of the difference between geometrical waves (obeying Snell's Law) and diffracted waves. *Top*: Ray tracing for *P* waves within the Earth, showing the shadow zone that exists between the *P* and *PKP* arrivals. *Bottom*: Diffracted *P* waves (*Pd*) that travel along the core-mantle boundary and leak back to the surface, arriving within the shadow zone and beyond.

basis for further determinations about the temperatures, compositions and core/mantle dynamics of the CMB region.

Pd and *Sd* waves have been observed since the start of the century (see *Sacks* [1966] and *Cleary* [1974] for discussions), though with the recognition of the complexity of of the CMB diffracted waveforms it has been through simulations with synthetic seismograms that recent studies have been able to model mantle properties. The results presented here were attained through comparison of the *Sd* and *Pd* arrivals with synthetic arrivals calculated with the reflectivity method, though our earlier studies used synthetics from normal mode summation [*Wysession and Okal*, 1988, 1989]. The reflectivity method was previously used by *Mula and Müller* [1980] and *Mula* [1981] in their studies of CMB diffracted waves.

Diffracted wave studies can involve investigations of both travel times and amplitudes, though we will concentrate here on the diffracted wave ray parameters as determined from the arrival times. The ray parameter (slowness) of a linear profile of diffracted arrivals is given by $p = dT/d\Delta = R_{CMB}/V_{CMB}$ (where T is the travel time, Δ the epicentral distance, R_{CMB} the radius of the CMB, and V_{CMB} the apparent velocity at the CMB) and is a direct indicator of the seismic velocities at the base of the mantle. However, p is only an *apparent* slowness and is a complicated function of D″ structure and particular earthquake-station geometries [*Chapman and Phinney*, 1972; *Mula and Müller*, 1980; *Wysession*, 1989, 1991], and therefore actual velocities at the base of the mantle cannot be simply taken from the ray parameter but must be inferred through comparisons with synthetic profiles. There are other precautions and corrections to be taken and made before D″ velocities can be inferred.

PROCEDURE

For our profiles we used the diffracted *P* and *S* arrivals at WWSSN and Canadian stations from 21 large earthquakes. This gave us 20 azimuthally independent *Pd* profiles and 12 *Sd* profiles, which each contain at least 4 stations (and as many as 10) along a similar azimuth that span from the start of the shadow zone to as great as 160°. Details are given in *Wysession* [1991].

The diffracted profiles are constrained to narrow azimuthal windows (a maximum of about 20°) so that the velocities of a particular strip through D″ are examined, and so that the downswing paths of all arrivals are essentially the same. This means that since we are measuring the slowness between arrivals and not absolute arrival times, we do not need to worry about source effects and mislocations, mantle heterogeneities (on the downswings), or slab diffraction [*Cormier*, 1989]. The *Sd* and *Pd* ray parameters, once given their necessary corrections, should be entirely a function the velocities within D″.

In an attempt to have the data and synthetics as comparable as possible, we correct the arrival times of the data for ellipticity using the relationships of *Jeffreys and Bullen*, 1970, and for mantle upswing path heterogeneities. The latter are calculated by ray tracing our waves through the full mantle 3-D tomographic velocity model of *Woodhouse and Dziewonski* [1987] and summing the velocity heterogeneities along the paths. The procedure is explained in detail in *Wysession and Okal* [1988, 1989].

The synthetic seismograms are generated using the reflectivity method, which gives easier access to the high frequency portions of the diffracted arrivals [*Wysession*, 1991], and are based on the algorithms of *Kennett* [1983]. The synthetic seismograms are generated for the radially symmetric PREM structure of *Dziewonski and Anderson* [1981], and are generated using the same focal mechanisms, path geometries and instrument responses as the data. Examples of the data and synthetic diffracted waves are given in Figure 2, which shows the *Sd* profile from Loyalty Island (Oct 7, 1966) to the Mid-East.

The data and synthetics are compared, and D″ velocities determined, on the basis of their apparent ray parameters (apparent slownesses), and we emphasize the necessity of this. The value of the measured ray parameter will be biased by the distance covered along the CMB, the geometry of stations used, the instrument frequency responses and the method used to determine it. One example of *Mula and Müller* [1980] used reflectivity synthetics to show that a particular apparent *P*-wave ray parameter of $p_{app} = 4.5$ s/deg, which would suggest an apparent velocity of $\alpha_{app} = 13$

km/s, actually was generated for an average D″ *P* velocity of α_{ave} = 13.74 km/s.

The slownesses represent the linear slope of the arrivals with increasing epicentral distance, as can be seen in Figure 2. For both the data and synthetics we determine the slownesses using two different robust techniques: peak maxima picks and multi-waveform cross-correlation. Though each adds bias into the data slownesses, this is recreated in the reflectivity synthetics. Details are explained in *Wysession and Okal* [1989]. The effects of the profile geometries, instrument responses and determination techniques can be seen in the ranges of slowness values for the synthetics. The ranges for the synthetic *Pd* slownesses were 4.51-4.59 s/deg (cross-correlation) and 4.49-4.55 s/deg (peak maxima), and for the Sd slownesses were 8.44-8.50 s/deg (cross-correlation) and 8.43-8.45 s/deg (peak maxima).

Once the data slownesses are determined relative to the synthetics, we can average the results for profiles that travel the same CMB paths. What we have is a measure of the percentage difference of the diffracted wave ray parameter in different parts of D″ relative to a PREM D″. What we would like is a measure of the percentage difference of the average velocities in different parts of D″ relative to the average velocity in PREM's D″. The apparent slownesses can be easily converted into apparent velocities by definition, but the translation of these apparent velocities into actual D″ velocities is very complicated. A determination of the radial structure of D″ is beyond the scope of this study, though eventually broadband arrays may give enough frequency amplitude information to invert for D″ radial velocities, much as is done in surface wave inversions.

It is possible, however, using the results of *Mula and Müller* [1980], to translate the apparent velocities into average velocities if a specific depth is determined for D″. Using 12 different velocity models that varied essentially only in the bottom 190 km of the mantle, *Mula and Müller* [1980] generated reflectivity synthetic diffracted *Pd* waves and determined the apparent ray parameters, which gave them the apparent D″ velocities. They found a striking linear correlation between these apparent velocities α_{app} and the *P* velocity averaged over the bottom 190 km of the mantle (α_{190}). Their conclusion was that if D″ was assumed to be 190 km thick, then $\alpha_{190} \propto 0.83\alpha_{app}$ (km/s). A similar result for shear waves yielded $\beta_{190} = \propto 0.65\beta_{app}$. These relationships are determined at a period of T = 20 sec, the approximate response peak of long period WWSSN instruments. In our discussions of average D″ velocities we will use these relationships to convert apparent velocities into D″ average velocities with the arbitrary assumption that D″ is 190 km thick, though it should be understood that the average velocities must increase if D″ is thinner, and must decrease if D″ is thicker.

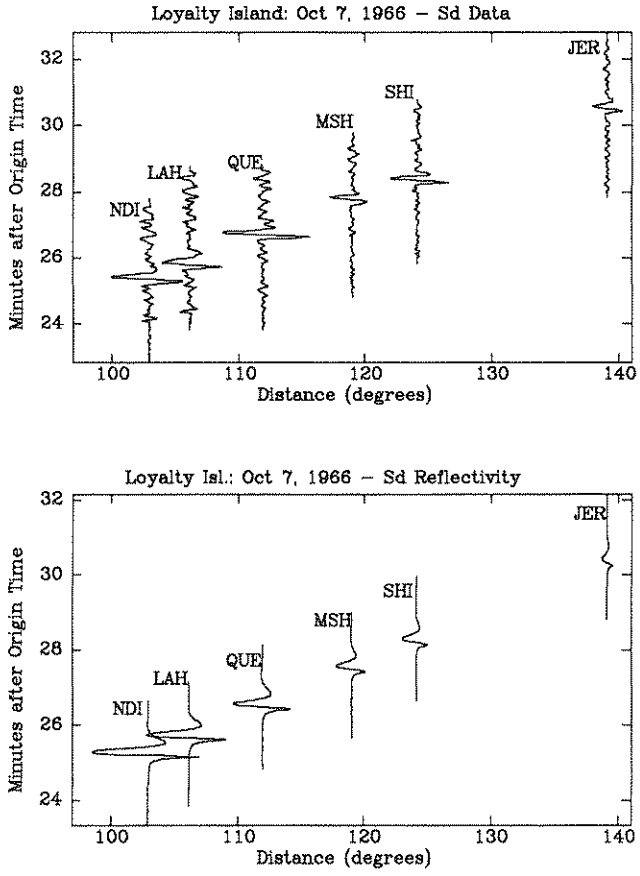

Figure 2. An example of the reflectivity synthetic seismograms, shown here modeling the diffracted *S* arrivals from the Loyalty Island 10/7/66 earthquake. Data are shown at the *top* and synthetics at the *bottom*.

Results and Discussion

The variations in averaged velocity, determined by differences between the data slownesses and PREM synthetics, is shown in Table 1. The actual range in individual apparent ray parameters was large: 4.44-4.80 s/deg for *Pd*, and 8.27-9.01 s/deg for *Sd*. When compared with the synthetics and averaged by region, the lateral variations were more moderate, but still amounted to several percent for both *P* and *S* velocities. As can be seen in Table 1, PREM does a fairly good job of serving as a reference model for the diffracted data, though there are roughly twice as many CMB regions that are slightly slower than PREM than are faster than PREM. It is not uncommon for a region to be faster or slower by about 1%, with the significant exception being under Indonesia. The regions we examined, including the path through Indonesia, displayed 4.0% and 3.9% lateral variation in α_{190} and β_{190}, respectively, implying that the level of heterogeneity for *P* and *S* is approximately the same. In our regional discussion it is important to bear in mind that for the 1 sec PREM velocities, α_{190} and β_{190} (over the 190 km at the base of the mantle) are 13.690 km/s and 7.264 km/s.

Certainly the most unusual region of the CMB that we found was underneath Northern Indonesia and Southeast Asia, as sampled from the diffracted wave profiles from the Tonga/Kermadec region across the Mid-East to the Mediterranean. There was very good coverage along this profile, with as many as eight stations well separated with a total distance range of up to 49°, and this allowed us to examine the first and second halves of the path sep-

arately, both retaining high quality profiles of several stations. The path profiles, when examined whole, showed no unusual velocities. Both α_{190} and β_{190} were nearly identical to those of PREM, with each being slightly slow (see Table 1). When separated, however, the second part showed slightly fast *P* and *S* velocities, but the first half had extremely slow velocities. We attempted to split up other profiles that had long distance ranges, and though in none of those cases did we find significant differences between the halves, their cross-correlograms were not good enough to include in the study.

Along the first half of the Tonga-to-Mid-East path, sampling CMB under Northern Indonesia, the apparent slowness was 3.8% slower than PREM for *P* waves and 4.7% slower for *S* waves. Again, using the assumptions above for a 190 km thick D″, this would imply the velocity anomalies to be $\Delta\alpha_{190}$ = -3.2% and $\Delta\beta_{190}$ = -3.1% (α_{190} = 13.25 km/s and β_{190} = 7.04 km/s). These are by far the lowest average D″ velocities that we have yet found. The results are very robust, found nearly identically in profiles from four earthquakes for *Pd* and three earthquakes for *Sd*. What makes this even more unusual is that the second half of these profiles, under Southeast Asia, is unusually fast, relative to PREM. The implied velocity anomalies along this segment were $\Delta\alpha_{190}$ = +0.7% and $\Delta\beta_{190}$ = +0.8%. This juxtaposition of slow and fast velocities also appears in tomographic studies that use non-diffracted arrivals, such as *Woodhouse and Dziewonski* [1987] (Model V3), *Tanimoto* [1987], and *Inoue et al.* [1990].

A possible geodynamic explanation for this may involve coupling with core flow. There is a strong correlation between our D″ velocities and the geomagnetically determined core flow model of *Voorhies* [1986] (and to a lesser extent, though still evident, *Bloxham* [1989]). Our slow velocity region beneath Indonesia sits right over one of the largest regions of CMB core upwelling in the *Voorhies* [1986] models, and the adjacent fast velocities are above the largest *Voorhies* [1986] region of downwelling. Thermochemically, a reduction in D″ seismic velocity would most likely be the result of increased temperature or iron content, and both of these would be expected above a core plume. If iron-silicate reactions [*Knittle and Jeanloz*, 1989b; *Jeanloz*, 1990] are occurring at the CMB, and liquid iron is seeping into the mantle through capillary action [*Stevenson*, 1986], then we would expect there to be both an increase in heat flux into the mantle and an increase in the amount of denser (and seismically slower) iron oxides in D″ above a region of vigorous core upwelling.

There is a difficulty in understanding why a correlation should exist between mantle and outer core features, when the core flow patterns are transitory in comparison to the longer times scales of mantle dynamics. Even though these core features under Indonesia and Southeast Asia have changed little over the last century and a half [*Bloxham and Jackson*, 1989], over much longer times scales we would require a dynamic coupling between the mantle and core. However, it is possible that a mantle anomaly may give rise to a preferential core flow, and cause a positive feed-back that will reinforce the mantle anomaly. Many of the studies of secular variation of core flow patterns do suggest the necessity of mantle-core coupling [*Bloxham and Gubbins*, 1987]. This could take the form of either gravitational coupling between density inhomogeneities, or topographic coupling, due to the pressure gradients in the core near CMB topography, both of which are discussed in *Jault and LeMouël* [1989, 1990] and *Bloxham and Jackson* [1991].

Electromagnetic coupling between the mantle and core was suggested by *Jeanloz* [1990] due to lateral variations in D″ electrical

TABLE 1. D″ Velocities Relative to PREM Averaged over 190 km and Inferred From the Apparent Slownesses of Diffracted P and S Wave Profiles

Number of Profiles	Path Description	CMB Region Sampled	ΔV_{190}
	Diffracted P		
1	Taiwan to the Eastern Americas	Arctic Ocean / northern Canada	+0.8%
3	Taiwan/Korea to the Western Americas	northwest North America	-1.0%
3	Indonesia to North America	North Pacific Rim	-0.9%
3	Tonga to North America	east central Pacific	-0.1%
1	Sandwich Islands to North America	northeast South America	-0.6%
3	South America to Europe/Asia	northeast Atlantic / Mediterranean	-1.0%
1	Tonga to Europe/Asia	northern Pacific	-0.3%
1	Indonesia to Europe	north central Asia	+0.6%
4	Tonga to Mid-East (whole)	Indonesia / Southeast Asia	-0.3%
4	Tonga to Mid-East (first part)	Indonesia	-3.2%
4	Tonga to Mid-East (second part)	Southeast Asia	+0.7%
	Diffracted S		
1	Burma to North America	Artic Ocean	-0.1%
1	Indonesia to Europe	north central Asia	-0.4%
3	Japan/Kuriles to Americas	northwest North America	+1.0%
3	Tonga to North America	east central Pacific	+0.5%
4	Tonga to Mid-East (whole)	Indonesia / Southeast Asia	-0.2%
3	Tonga to Mid-East (first part)	Indonesia	-3.1%
3	Tonga to Mid-East (second part)	Southeast Asia	+0.8%

conductivity of more than 11 orders of magnitude. Metal-rich heterogeneities in D″ would pin the magnetic field lines from the core, either distorting the image of flow patterns or controlling core flow near the CMB. The metal-rich D″ rock needed to maintain this electromagnetic coupling, FeO and FeSi created from iron-silicate reactions and locally aggregated through intra-D″ convective sweeping [*Davies and Gurnis*, 1986; *Zhang and Yuen*, 1988; *Hansen and Yuen*, 1989; *Sleep*, 1988], would have significantly slower velocities than perovskite, and only small additional amounts would be required to give us the slow D″ velocities we see under Indonesia. So while the correlation between seismic and geomagnetic images may be coincidental, it is not unlikely that this is an indication of significant coupling between the mantle and core.

It is interesting to note that the *P* and *S* velocities do not always differ from PREM in the same way. In *Wysession and Okal* [1988, 1989] we found that the CMB region underneath Alaska and Canada, along the northern rim of the Pacific, had relatively fast *S* velocities and relatively slow *P* velocities, and in quantifying this with the reflectivity synthetics we still found this to be true. The three *Sd* profiles from Japan and the Kurile Trench to the Americas had a velocity anomaly of $\Delta\beta_{190} = +1.0\%$, whereas for three similar profiles from Taiwan/Korea to the Americas (as well as three from Indonesia to North America) the *P* anomaly was $\Delta\alpha_{ave} = -1.0\%$. The fast shear velocities occur in the same region where *ScS*-precursor studies like *Lay and Helmberger* [1983] and *Young and Lay* [1990] have found evidence of a very high *S*-velocity zone, and are also seen in the tomographic shear velocity models of *Tanimoto* [1987] and *Grand* [pers. comm., 1991]. The same high velocity zone has not been seen there from *PcP* precursors, and in fact tomographic *P* velocity models [*Morelli and Dziewonski*, 1987; *Inoue et al.*, 1990] also find slightly slower anomalies. The occurrence of fast shear velocities at the base of the mantle beneath the rim of the Northern Pacific would not be surprising under the geodynamic circumstances. Subduction has been occurring for a long time there, and because the absolute plate motion of the North America/Pacific trench is very slow - on the order of 1 cm/yr [*Gripp and Gordon*, 1990] - there has been a lot of cold material that has been put into the mantle above where our diffracted waves sample the CMB. If the slabs penetrated into the lower mantle, or if convection limited to the upper mantle was thermally coupled to the lower mantle, then we might expect to see an accumulation of the mantle dregs there at the CMB [*Ringwood*, 1975; *Hofman and White*, 1982].

Poisson Ratio

The fact that *P* velocities here are slow, however, suggests that the shear and bulk elastic moduli here are behaving in a manner different from D″ rock elsewhere, again suggesting a different chemical signature. We can quantify this behavior with the Poisson ratio, ν, which equals 0.5 for a liquid but decreases with more pronounced rigidity. As we will show, variations in temperature and pressure can give rise to changes in ν. For the Japan-Americas path the reversal of velocity variations leads to a Poisson ratio of $\nu_0 = 0.292$. This is 4% less than for PREM, which yields $\nu_{190} = .304$. These values are listed in Table 2, along with those for the other CMB regions for which we had both *Pd* and *Sd* coverage. While the paths from Tonga, to North America and both halves to the Mid-East, do not display any variation in ν, the Indonesia to Europe path, sampling D″ beneath Northern Siberia, shows an increase in ν because the shear velocity is slow but the *P* velocity is fast. While the 5.5% variation seen in the Poisson ratios of our profiles does not seem large given the possible errors in P and S velocities (1% errors for V_p and V_s would suggest approximately 3.5% errors in ν), it is significant because contaminating factors (source and mantle heterogeneities, conversions from slownesses to average velocities) will effect V_p and V_s in similar manners.

TABLE 2. Velocity Results for Dual *P/S* Coverage, Including Poisson Ratios

Path Description	α_{190}, km/s	β_{190}, km/s	ν
PREM	13.69	7.26	0.304
Taiwan/Japan to Western Americas	13.55	7.34	0.292
Indonesia to Europe	13.77	7.23	0.309
Tonga to North America	13.68	7.30	0.301
Tonga to Mid-East (first part)	13.25	7.04	0.303
Tonga to Mid-East (second part)	13.79	7.32	0.304

Thermal gradient

One explanation for the 5.5% range we see in the D″ Poisson ratio could be a lateral variation in the thermal expansivity due to slight compositional changes, in connection with a rapidly increasing thermal gradient. D″ probably sees a departure from a mid-mantle adiabat of around 0.5°C/km to as much as 20°C/km by the time the core is reached, much like the Earth's surface. And the top of the lithosphere, the other major thermal boundary layer in the Earth, also displays strong variations in ν [*Clarke and Silver*, 1991]. Extending the derivations of *Stacey and Loper* [1983] and *van Loenen* [1988] to include the shear modulus terms, if we expand the vertical *P* and *S* velocity gradients into their fundamental thermoelastic constituents, we go from

$$\frac{dv_s}{dz} = \left[\frac{\partial v_s}{\partial T}\right]_P \frac{dT}{dz} + \left[\frac{\partial v_s}{\partial P}\right]_T \frac{dP}{dz} \qquad (1)$$

and

$$\frac{dv_p}{dz} = \left[\frac{\partial v_p}{\partial P}\right]_T \frac{dP}{dz} + \left[\frac{\partial v_p}{\partial T}\right]_P \frac{dT}{dz} \qquad (2)$$

to

$$\frac{dv_s}{dz} = \left\{\frac{1}{2v_s\rho}\left[\frac{\partial \mu}{\partial T}\right]_P + \frac{\alpha v_s}{2}\right\}\frac{dT}{dz} + \qquad (3)$$

$$+ \frac{g}{2v_s}\left\{\left[\frac{\partial \mu}{\partial P}\right]_T - \frac{\rho v_s^2}{K_s}(1 + \gamma_{th}\alpha T)\right\}$$

and

$$\left[\frac{dv_p}{dz}\right] = \frac{1}{2v_p\,\rho}\left\{\left[\frac{\partial K_S}{\partial T}\right]_P + \frac{4}{3}\left[\frac{\partial \mu}{\partial T}\right]_P + v_p^2\,\rho\alpha\right\}\frac{dT}{dz} + \quad (4)$$

$$+\frac{g}{2v_p}\left\{\left[\frac{\partial K_S}{\partial P}\right]_T + \frac{4}{3}\left[\frac{\partial \mu}{\partial P}\right]_T - \frac{\rho v_p^2}{K_S}(1+\gamma_{th}\alpha T)\right\}$$

where v_S is the S velocity, v_P the P velocity, z the depth, P the pressure, T the temperature, μ the shear modulus, K_S the adiabatic incompressibility, ρ the density, g the acceleration of gravity, γ_{th} the thermal Grüneisen ratio, and α the coefficient of thermal expansion. An interesting result occurs when reasonable lower mantle values are inserted, shown in Figures 3 and 4 [values were taken from *Dziewonski and Anderson*, 1981; *Lay*, 1989; *Isaak et al.*, 1989; *Knittle at al.*, 1986; *Hemley et al.*, 1987; *Yeganeh-Haeri et al.*, 1989]. The only difference between the two is that in Figure 4 the thermal expansivity is increased from 1.3×10^{-5} K^{-1} to 4.0×10^{-5} K^{-1}, and $\partial K_S/\partial T$ from -0.015 GPa/K to -0.035 GPa/K. Such a change is not unreasonable, as there have been a wide range of experimental values put forward, and the temperature derivatives of elastic moduli at 3000 K and 136 GPa are certainly not known to within a factor of 2. These changes have reversed the order in which the P and S velocity gradients become negative with increasing thermal gradients. In the case of Figure 3 the S velocity gradient becomes negative first, causing there to be a region along the thermal gradient axis where the P velocities would still be increasing but the S velocities would be decreasing. Though this linear approximation is really only meaningful at a particular point in temperature/pressure space, it can serve to demonstrate that since the thermal gradient will be increasing with depth in D″ there would be a physical layer within D″, corresponding to this region along the thermal gradient axis, where the P and S velocity gradients would be reversed. In Figure 4 just the opposite occurs - there will be a layer within D″ where the S velocities will still be increasing but the P velocities will be decreasing. Beneath these layers both velocities will decrease as the much hotter iron core draws near.

The implication here is that if we were to travel laterally along the CMB between regions whose materials had different physical properties, such as differing amounts of perovskite and magnesiowüstite, we might expect the P and S velocities to vary in different ways. If there really is as much variation in the thermal expansivity in D″ as there is in laboratories at the surface, then we could expect lateral variations of the increase in the thermal gradient to be driving the differences between P and S velocities.

D″ Equations of State

One avenue of modeling seismic velocities in D″ is through the use of equations of state of mineral phases that we know are stable at CMB conditions and presume comprise a significant part of the lower mantle. This method uses the standard temperature and pressure (STP) elastic moduli and their temperature and pressure derivatives of the iron and magnesium end members of perovskite and magnesiowüstite, and calculates the elastic moduli and density at CMB conditions. This allows us to see what kinds of thermochemical variations are necessary in order to explain the seismic lateral heterogeneity, such as the anomalously slow D″ velocities underneath Indonesia and the adjacent region of fast velocities.

Our investigations have used a third-order Birch-Murnaghan equation of state in order to model our D″ velocity anomalies [*Birch*, 1952; *Bina and Helffrich*, 1991].CMB velocities are cal-

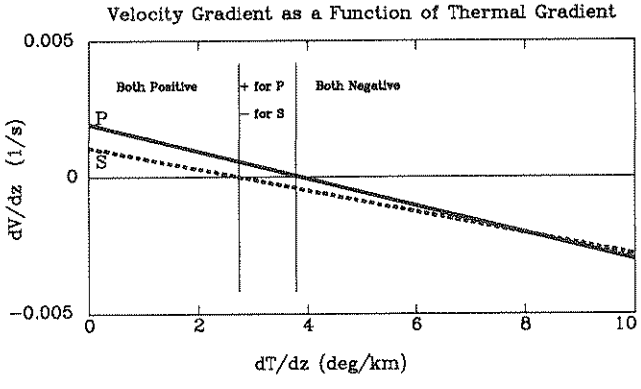

Figure 3. An example of the P and S velocity gradients as functions of the thermal gradient at the base of the mantle. The thermoelastic parameters used for the calculation are K_S = 685 GPa; μ = 291 GPa; $\alpha = 1.3 \times 10^{-5}$ K^{-1}; $\partial K_S/\partial T$ = -0.015 GPa/K; $\partial\mu/\partial T$ = -0.035 GPa/K; K_S' = 4.0; μ' = 1.9; T = 3000 K (sources are given in the text). Note that the shear velocity gradient becomes negative before the P velocity gradient, creating a layer in D″ in which P velocities are still increasing but S velocities are decreasing.

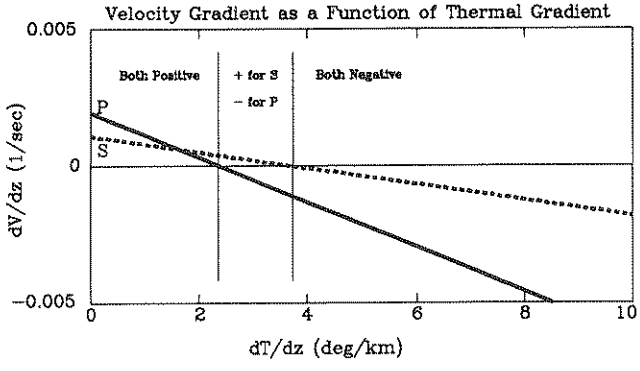

Figure 4. An example of the P and S velocity gradients as functions of the thermal gradient at the base of the mantle. The thermoelastic parameters used for the calculation are K_S = 685 GPa; μ = 291 GPa; $\alpha = 4.0 \times 10^{-5}$ K^{-1}; $\partial K_S/\partial T$ = -0.035 GPa/K; $\partial\mu/\partial T$ = -0.035 GPa/K; K_S' = 4.0; μ' = 1.9; T = 3000 K (sources are given in the text).Note that in this case the P velocity gradient becomes negative before the S velocity gradient, creating a layer in D″ in which S velocities are still increasing but P velocities are decreasing. This is the opposite of the case represented in Figure 3.

culated by starting with the elastic moduli and their derivatives for the iron and magnesium end members of perovskite and magnesiowüstite, listed in Table 3, and then making the independent temperature and pressure corrections as demonstrated in *Bina and Silver* [1990]. While these initial values are difficult to obtain experimentally and are therefore subject to change with future research, they will at least give us an order of magnitude understanding of the sensitivity of D″ velocities to changes in temperature and composition. For any combination of minerals, the resulting velocities calculated for each are combined according to the molar proportions desired. We make the assumption that bulk material velocities vary linearly with the volume proportions of the minerals include, and while this assumption may not be perfectly accurate, it is much less of a worry that the assumptions we make for the starting STP parameters of (Mg, Fe)SiO_3 perovskite and (Mg, Fe)O magnesiowüstite.

Because of uncertainties in the thermoelastic parameters we do not present absolute values but rather the percentage variations in velocities due to changes in temperature and composition. The results of the computations are shown in Tables 4-6, assuming an Fe-Mg partitioning coefficient between perovskite (Pv) and magnesiowüstite (Mw) of 0.1 [*Bell et al.*, 1979; *Ito and Yamada*, 1982] and a D″ pressure of 135 GPa. We used an initial model of pyrolitic composition (Pv/(Pv+Mw) = 2/3) with a magnesium/metal ratio of 0.9 at a temperature of 3500 K and varied these three parameters. Given the particular set of thermoelastic parameters we used, the seismic velocities were sensitive to both changes in temperatures and iron/magnesium ratios, though much less so for Pv/Mw deviations.

In Table 4 we see that a 1% variation in seismic velocities could be explained by lateral variations of approximately 200° C for *P* and 300° C for *S*. The effect of changes in temperature on seismic velocities is most likely significantly less in D″ than at the surface, because the temperature derivative of the thermal expansivity is much smaller [*Mao et al.*, 1991] and perovskite and magnesiowüstite seem stable and far from their solidi [*Knittle and Jeanloz*, 1989*a*, 1991; *Vassiliou and Ahrens*, 1982] under D″conditions. Nonetheless, most of the seismic variations from PREM for our profiles are on the order of approximately 1%, and if lateral variations in temperature over the top 200 km of the earth are any indication, then temperature could be a dominant factor driving the seismic heterogeneities. Excluding the region under Indonesia, the ranges of anomalies from our averaged profiles correspond here to $\Delta T \approx 400°$ C for *P* and $\Delta T \approx 500°$ C for *S*. These seem slightly larger than one might reasonably allow, but probably not by more than a factor of two.

However, the D″ velocity low under Indonesia, more than 3% slow for both *P* and *S* velocities, cannot be explained just as a thermal anomaly, but is well modeled by an increase in iron, as is shown in Table 5. The commonly accepted Mg/(Mg+Fe) ratio for the lower mantle is approximately 0.9, but a value of 0.7 would satisfy the Indonesian low. In actuality we would not even need quite this much iron, because regions of high iron content would be areas where the products of mantle-core reactions were swept together, and these regions would experience a thermal anomaly from the inclusion of so much core material. Both an increase in heat flux from the core and iron percolation into the mantle would be expected to increase where core liquid was flowing up and against the CMB, if it could be held in one place for a significant amount of time. So the scenario for the D″ area under Indonesia sitting over an upwelling core plume [*Voorhies*, 1986], held in

TABLE 3. Thermoelastic Parameters Used for the Equation of State Velocity Calculations

Parameter	$MgSiO_3$	$FeSiO_3$	MgO	FeO
V_0	24.46[a]	25.49[a]	11.25[a]	12.25[a]
K_{S0}, GPa	268[b]	268[b]	163[a]	180[a]
K'_{S0}	4.0[b,c]	4.0[b,c]	4.1[a]	3.6[a]
δ_S	2.7[d]	2.7[d]	2.8[e]	3.0[f]
$\alpha_0{}^g$ ($\times 10^{-5}$), K^{-1}	4.9[c]	4.9[c]	4.7[e]	5.9[e,a]
$d\alpha/dT^h$ ($\times 10^{-8}$), K^{-2}	1.7[c]	1.7[c]	1.04[e]	2.2[e,a]
$d\alpha/dT^l$ ($\times 10^{-8}$), K^{-2}	1.6[c]	1.6[c]	0.8[e]	1.7[e,a]
μ, GPa	185[j]	185[j]	132[e]	118[k]
μ'	1.9[j]	1.9[j]	2.5[l]	2.5[l]
$d\mu/dT$ ($\times 10^{-4}$), GPa/K	-3.3[j]	-3.3[j]	-2.5[e]	-2.5[e]

[a] *Jeanloz and Thompson* [1983].
[b] *Knittle and Jeanloz* [1987].
[c] *Mao et al.* [1991].
[d] *Bukowinski and Wolf* [1990].
[e] *Isaak et al.* [1989].
[f] *Sumino and Anderson* [1984].
[g] determined at 1300 K.
[h] linear value for $T < 1300$ K.
[l] linear value for $T > 1300$ K.
[j] *Yeganehi-Haeri et al.* [1989].
[k] *Jeanloz* [1990].
[l] *Agnon and Bukowinski* [1988].

TABLE 4. Velocity Variations Due to Changes in Temperature

Temperature, K	ΔV_P	ΔV_S	Δv
3100	+1.6%	+1.1%	+1.6%
3300	+0.8%	+0.6%	+0.9%
3500	-----	-----	-----
3700	-0.9%	-0.6%	-1.0%
3900	-1.7%	-1.2%	-2.0%

TABLE 5. Velocity Variations Due to Mg/Fe Variations

Mg/(Mg+Fe)	ΔV_P	ΔV_S	Δv
1.0	+1.9%	+1.8%	+0.3%
0.9	-----	-----	-----
0.8	-1.8%	-1.7%	-0.3%
0.7	-3.5%	-3.3%	-0.5%

TABLE 6. Velocity Variations Due to Oxide/Silicate Ratio Changes

Model	ΔV_P	ΔV_S	Δv
Pv	+0.2%	-0.9%	+3.6%
2Pv + Mw	-----	-----	-----
Pv + 2Mw	-0.1%	+1.6%	-5.8%

place by electromagnetic coupling due to the pinning of magnetic field lines by conductive iron-rich rock [*Jeanloz*, 1990], would be compatible with the *P* and *S* seismic anomaly we see there.

Changes in the relative amounts of perovskite and magnesiowüstite were not as significant as with the Mg/Fe ratio, as is seen in Table 6. Modest changes in shear velocity require very large Pv/Mw variations, and the *P* velocities are insensitive to it, given our initial parameters. Even though the shear velocity of (Mg, Fe)O is much less than for (Mg, Fe)SiO_3 at the surface, in our calculations this difference becomes less pronounced at great depths because recent experimental results suggest that the temperature and pressure derivatives of the shear moduli are more favorable for faster Mw than Pv [*Agnon and Bukowinski*, 1988; *Isaak et al.*, 1989; *Yeganeh-Haeri et al.*, 1989]. It is interesting, however, that for the case of Pv/Mw variations the Poisson ratio varies significantly, suggesting that in areas like the CMB under Northern North America, where *S* velocities are fast but *P* velocities slightly slow, this kind of variation may play a role. It is interesting to compare this experiment with the variations in temperature and Mg/Fe ratio - all three affect the *P* and *S* velocities at very different relative rates.

While the comparisons drawn here between seismic anomalies and thermochemical variations are highly speculative, and the correlations will change greatly as future experimental work is done, they represent the direction that CMB research will be taking in the future. As seismic (as well as geomagnetic and geodynamic) models become more refined, and as experimental mineral physics continues to advance methods to simulate deep earth conditions, we will eventually be able to map out the thermal and chemical variations at the base of the mantle and develop a full understanding of the coupling between the earth's core and mantle. There are certainly many other factors involved of which we have not taken account: additional phases such as SiO_2 stishovite may be present in significant amounts, anisotropy may be affecting our seismic velocities, etc. But CMB research is on the verge of having the insight to know what to look for and the resolution with which to see it

Acknowledgments. We would like to thank Andrea Morelli, Toshiro Tanimoto and John Woodhouse for the use of their respective tomographic mantle models, and Tim Clarke for introducing the reflectivity method. We also thank two anonymous reviewers for their comments. This research was partially supported by NSF grant EAR-84-05040.

REFERENCES

Agnon, A., and M. S. T. Bukowinski, High pressure shear moduli - a many-body model for oxides, *Geophys. Res. Lett., 15*, 209-212, 1988.

Bell, P. M., T. Yagi, and H.-K. Mao, Iron-magnesium distribution coefficients between spinel [$(Mg,Fe)_2SiO_4$], magnesiowüstite [(Mg,Fe)O], and perovskite [$(Mg,Fe)SiO_3$], Vol. 78, Year Book Carnegie Inst. Washington, 618-621, 1979.

Bina, C. R., and G. R. Helffrich, Calculation of elastic properties from thermodynamic equation of state principles, *Ann. Rev. Earth Planet. Sci.*, in prep, 1991.

Bina, C. R., and P. G. Silver, Constraints on lower mantle composition and temperature from density and bulk sound velocity profiles, *Geophys. Res. Lett., 17*, 1153-1156, 1990.

Birch, F., Elasticity and constitution of the Earth's interior, *J. Geophys. Res., 57*, 227-286, 1952.

Bloxham, J., Simple models of fluid flow at the core surface derived from geomagnetic field models, *Geophys. J. Int., 99*, 173-182, 1989.

Bloxham, J., and D. Gubbins, Thermal core-mantle interactions, *Nature, 325*, 511-513, 1987.

Bloxham, J., and A. Jackson, Simultaneous stochastic inversion for geomagnetic main field and secular variation, 2, 1820-1980, *J. Geophys. Res., 94*, 15,753-15,769, 1989.

Bloxham, J., and A. Jackson, Fluid flow near the surface of Earth's outer core, *Rev. of Geophys., 29*, 97-120, 1991.

Bukowinski, M. S. T., and G. H. Wolf, Thermodynamically consistent decompression: Implications for lower mantle composition, *J. Geophys. Res., 95*, 12,583-12,593, 1990.

Chapman, C. H., and R. A. Phinney, Diffracted seismic signals and their numerical solution, *Methods in Computational Physics, 12*, 165-230, 1972.

Chopelas, A., and R. Boehler, Thermal expansion measurements at very high pressure, systematics, and a case for a chemically homogeneous mantle, *Geophys. Res. Lett., 16*, 1347-1350, 1989.

Clarke, T. J., and P. G. Silver, A procedure for the systematic interpretation of body wave seismograms - I. Application to Moho depth and crustal properties, *Geophys. J. Int., 104*, 41-72, 1991.

Cleary, J. R., The D'' region, *Phys. Earth Planet. Inter., 30*, 13-27 1974.

Cohen, R. E., Elasticity and equation of state of $MgSiO_3$ perovskite. *Geophys. Res. Lett., 14*, 1053-1056, 1987.

Cormier, V. F., Slab diffraction of *S* waves, *J. Geophys. Res., 94*, 3006-3024, 1989.

Davies, G. F., and M. Gurnis, Interaction of mantle dregs with convection: lateral heterogeneity at the core-mantle boundary, *Geophys. Res. Lett., 13*, 1517-1520, 1986.

Dziewonski, A. M., and D. L. Anderson, Preliminary reference earth model, *Phys. Earth Planet. Inter., 25*, 297-356, 1981.

Fei, Y., H.-K. Mao, and B. O. Mysen, Experimental determination of element partitioning and calculation of phase relations in the MgO-FeO-SiO_2 system at high pressure a high temperature, *J. Geophys. Res., 96*, 2157-2170, 1991.

Gripp, A. E., and R. G. Gordon, Current plate velocities relative to the hotspots incorporating the NUVEL-1 global plate motion model, *Geophys. Res. Lett., 17*, 1109-1112, 1990.

Hansen, U., and D. A. Yuen, Dynamical influences from thermal-chemical instabilities at the core-mantle boundary, *Geophys. Res. Lett., 16*, 629-632, 1989.

Hemley, R. J., M. D. Jackson, and R. G. Gordon, Theoretical study of the structure, lattice dynamics, and equations of state of perovskite-type $MgSiO_3$ and $CaSiO_3$, *Phys. Chem. Minerals, 14*, 2-12, 1987.

Hofman, A. W., and W. M. White, Mantle plumes from ancient oceanic crust, *Earth Planet. Sci. Lett., 57*, 421-436, 1982.

Inoue, H., Y. Fukao, K. Tanabe, and Y. Ogata, Whole mantle *P*-wave travel time tomography, *Phys. Earth Planet. Int., 59*, 294-328, 1990.

Isaak, D. G., O. L. Anderson, and T. Goto, Measured elastic mod-

uli of single-crystal MgO up to 1800 K, *Phys. Chem. Minerals, 16*, 704-713, 1989.

Ito, E., and H. Yamada, *Stability relations of silicate spinels, ilmenites and perovskites*, In High-Pressure Research in Geophysics, ed. S. Akimoto and M. H. Manghnani, 405-419, 1982.

Jault, D., and J.-L. LeMouël, The topographic torque associated with a tangentially geostrophic motion at the core surface and inferences on the flow inside the core, *Geophys. Astrophys. Fluid Dyn., 48*, 273-296, 1989.

Jault, D., and J.-L. LeMouël, Core-mantle boundary shape: Constraints inferred from the pressure torque acting between the core and mantle, *Geophys. J. Int., 101*, 233-241, 1990.

Jeanloz, R., The nature of the Earth's core, *Annu. Rev. Earth Planet. Sci., 18*, 357-386, 1990.

Jeanloz, R., and A. B. Thompson, Phase transitions and mantle discontinuities, *Rev. Geophys. Space Phys., 21*, 51-74, 1983.

Jeffreys, H., and K. E. Bullen, *Seismological tables*, 50 pp., Brit. Assoc. Adv. Science, London, 1970.

Kennett, B. L. N., *Seismic Wave Propagation in Stratified Media*, Cambridge University Press, Cambridge, MA, 1983.

Knittle, E., and R. Jeanloz, Synthesis and equation of state of (Mg, Fe)SiO_3 perovskite to over 100 GPa, *Science, 235*, 668-670, 1987.

Knittle, E., and R. Jeanloz, Melting curve of (Mg,Fe)SiO_3 perovskite to 96 GPa: evidence for a structural transition in lower mantle melts, *Geophys. Res. Lett., 16*, 421-424, 1989*a*.

Knittle, E., and R. Jeanloz, Simulating the core-mantle boundary: n experimental study of high-pressure reactions between silicates and liquid iron, *Geophys. Res. Lett., 16*, 609-612, 1989*b*.

Knittle, E., and R. Jeanloz, The high pressure phase diagram of $Fe_{0.94}O$: A possible constituent of the Earth's core, *J. Geophys. Res., 96*, 16169-16180, 1991.

Knittle, E., R. Jeanloz, and G. L. Smith, Thermal expansion of silicate perovskite and stratification of the earth's mantle, *Nature, 319*, 214-216, 1986.

Lay, T., Structure of the core-mantle transition zone: a chemical and thermal boundary layer, *Eos Trans. AGU, 70*, 49, 1989.

Lay, T., and D. V. Helmberger, A lower mantle *S*-wave triplication and the velocity structure of D″, *Geophys. J. R. astron. Soc., 75*, 799-837, 1983.

Mao, H. K., R. J. Hemley, Y. Fei, J. F. Shu, L. C. Chen, A. P. Jephcoat, Y. Wu, and W. A. Bassett, Effect of pressure, temperature and composition on lattice parameters and density of (Fe,Mg)SiO_3-perovskites to 30 GPa, *J. Geophys. Res., 96*, 8069-8079, 1991.

Mondt, J. C., *SH* waves: Theory and observations for epicentral distances greater than 90 degrees, *Phys. Earth Planet. Inter., 15*, 46-59, 1977.

Morelli, A., and A. M. Dziewonski, Topography of the core-mantle boundary and lateral heterogeneity of the liquid core, *Nature, 325*, 678, 1987.

Mula, A. H., Amplitudes of diffracted long-period *P* and *S* waves and the velocities and Q structure at the base of the mantle, *J. Geophys. Res., 86*, 4999-5011, 1981.

Mula, A. H., and G. Müller, Ray parameters of diffracted long period *P* and *S* waves and the velocities at the base of the mantle, *Pure Appl. Geophys., 118*, 1270-1290, 1980.

Ringwood, A., *Composition and petrology of the Earth's mantle*, McGraw-Hill, New York, 1975.

Sacks, S., Diffracted waves studies of the earth's core: 1. Amplitudes, core size, and rigidity, *J. Geophys. Res., 71*, 1173-1181, 1966.

Sleep, N. H., Gradual entrainment of a chemical layer at the base of the mantle by overlying convection, *Geophys. J. R. astron. Soc., 95*, 437-447, 1988.

Stacey, F. D., and D. E. Loper, The thermal boundary-layer interpretation of D" and its role as a plume source, *Phys. Earth Planet. Interiors, 33*, 45-55, 1983.

Stevenson, D. J., On the role of surface tension in the migration of melts and fluids, *Geophys. Res. Lett., 13*, 1149-1152, 1986.

Sumino, Y., and O. L. Anderson, Elastic constants of minerals, In *CRC Handbook of Physical Properties of Rocks, Volume III*, ed. R. S. Carmichael, Boca Raton, Florida: CRC Press, Inc., 39-138, 1984.

Tanimoto, T., The three-dimensional shear wave structure in the mantle by overtone waveform inversion - I. Radial seismogram inversion, *Geophys. J. R. astron. Soc., 89*, 713-740, 1987.

van Loenen, P. M, S velocity at the base of the mantle from diffracted SH waves recorded by the NARS array, M.Sc. Thesis, Department of Theoretical Geophysics, Utrecht, 1988.

Vassiliou, M. S., and T. J. Ahrens, The equation of state of $Mg_{0.6}Fe_{0.4}O$ to 200 GPa, *Geophys. Res. Lett., 9*, 127-130, 1982.

Voorhies, C. V., Steady flows at the top of Earth's core derived from geomagnetic field models, *J. Geophys. Res., 91*, 12,444-12,466, 1986.

Woodhouse, J. H., and A. M. Dziewonski, Models of the upper and lower mantle from waveforms of mantle waves and body waves, *Eos Trans. AGU, 68*, 356-357, 1987.

Wysession, M. E., Diffracted seismic waves and the dynamics of the core-mantle boundary, Ph.D. Thesis, Northwestern University, Evanston, Illinois, 190 pp, 1991.

Wysession, M. E., and E. A. Okal, Evidence for lateral heterogeneity at the core-mantle boundary from the slowness of diffracted *S* profiles, *AGU Monog., 46*, 55-63, 1988.

Wysession, M. E, and E. A. Okal, Regional analysis of D″ velocities from the ray parameters of diffracted *P* profiles, *Geophys. Res. Lett., 16*, 1417-1420, 1989.

Yeganeh-Haeri, A., D. J. Weidner, and E. Ito, Elasticity of $MgSiO_3$ in the perovskite structure, *Science, 243*, 787-789, 1989.

Young, C. J., and T. Lay, The core mantle boundary, *Ann. Rev. Earth Planet. Sci., 15*, 25-46, 1987.

Young, C. J., and T. Lay, Multiple phase analysis of the shear velocity structure in the D″ region beneath Alaska, *J. Geophys. Res., 95*, 17,385-17,402, 1990.

Zhang, S., and D. A. Yuen, Dynamical effects on the core-mantle boundary from depth-dependent thermodynamical properties of the lower mantle, *Geophys. Res. Lett., 15*, 451-454, 1988.

C. R. Bina and E. A. Okal, Department of Geological Sciences, Northwestern University, Evanston, IL 60208.

M. E. Wysession, Department of Earth and Planetary Sciences, Washington University, Campus Box 1169, One Brookings Dr., St. Louis, MO 63130-4899.